Electronic Supplementary Material (ESI) for ChemComm.

Resolving Alternative Structure Determinations of Indapamide Using ^{13}C Solid-State NMR: Supplementary Information

Caitlin L. Evans, Ivana R. Evans and Paul Hodgkinson

Department of Chemistry, Durham University, Stockton Road, Durham, DH1 3LE, UK

TABLE OF CONTENTS

1. Powder X-Ray Diffraction Simulated Patterns.

Simulations were calculated using Mercury (Version 5.3.0)[1].

(a) VAGKUM

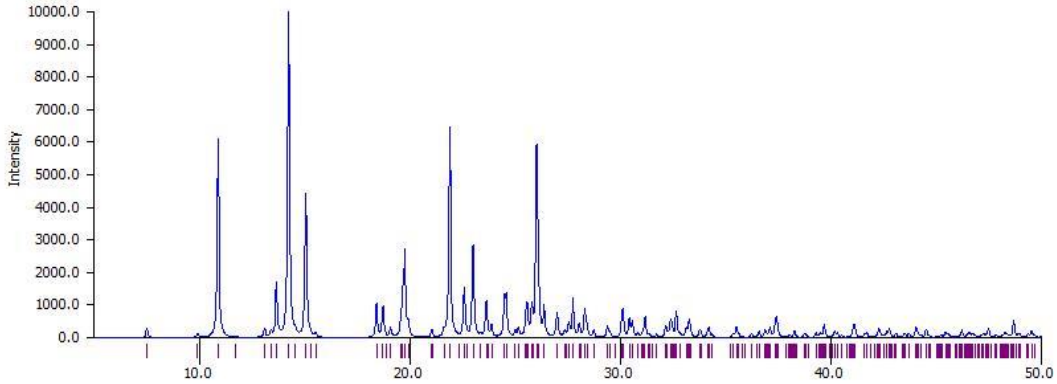

(b) WOCPEM

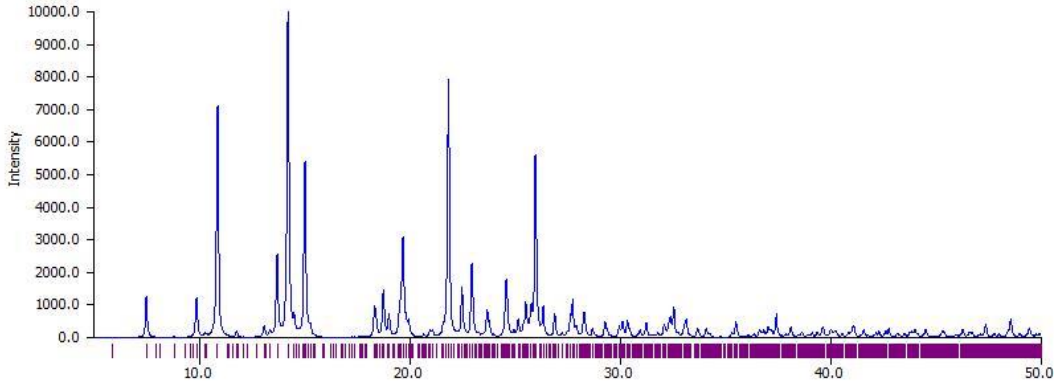

(c) WOCPEM NEW

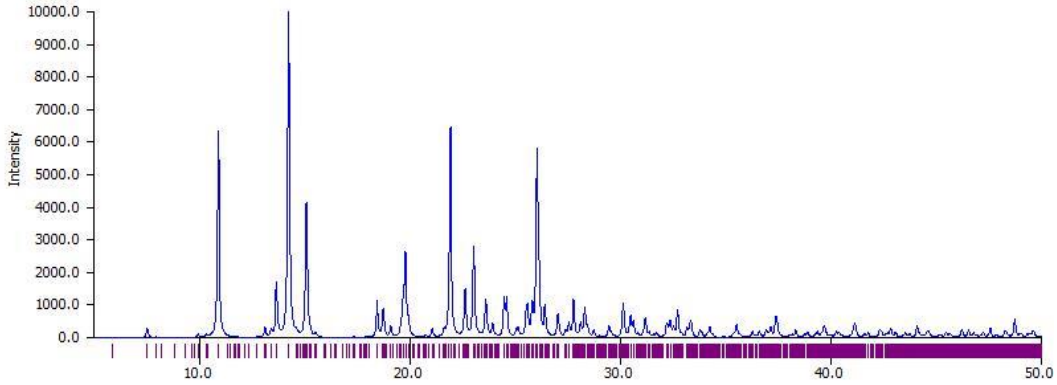

Figure S1: Simulated PXRD patterns for CSD structures with reference codes (a) **VAGKUM**[2], (b) **WOCPEM**[3] alongside (c) simulated pattern from this work, **WOCPEM NEW**. Tick marks indicate predicted reflection positions (systematically absent reflections are excluded).

PXRD data was performed on a Bruker D8 Advance diffractometer equipped with Cu $K\alpha_{1,2}$ source (λ = 1.5418 Å), Lynx-Eye Soller PSD detector and variable slits. The sample was lightly ground and sprinkled onto Si slides covered with a thin layer of Vaseline. The PXRD pattern was collected at room temperature for 60 minutes over a 2θ range of 1–55° using a step size of 0.02°.

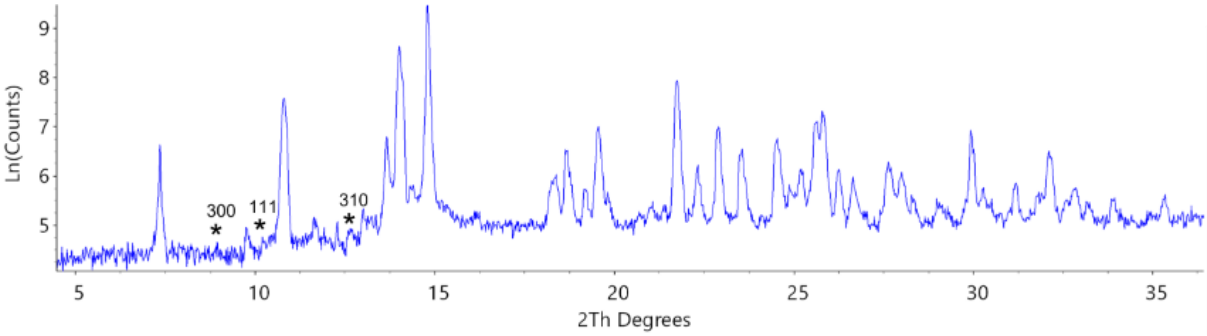

Figure S2: Truncated experimental PXRD pattern with the positions and very weak intensities for the (300), (310) and (111) reflections of the **WOCPEM** unit cell highlighted with an asterisk (*). Data visualised using Topas Academic software.[4]

2. Analysis of Geometry Optimisation

As argued by van de Streek and Neumann[5] and Widdifield et al.[6] an RMSD value on the atomic displacements (excluding H atoms) during geometry optimisation above 0.25 Å (for a non-disordered structure) indicates that a structure may be problematic. Individual atomic displacements above 0.25 Å also suggest poorly placed atoms, especially H.[6]

For **FOCCAD**, significant displacements were observed which reinforces our choice to omit it from further study. The overall displacements for the **VAGKUM** are large (albeit below 0.25 Å), but it is difficult to read too much into these values given the unphysical nature of calculations. Both **WOCPEM** and **WOCPEM NEW** show modest overall displacements on geometry optimisation. Note, however, that there are significant individual displacements for both **WOCPEM** structures; the displaced atoms are in one of the water molecules (**WOCPEM**) or a sulfonamide proton (**WOCPEM NEW**), both of which are involved in hydrogen bonding between water and sulfonamide. This is likely to reflect dynamic disorder on the water molecule (see the relatively large ADPs for the water molecule atoms in Fig. S5). The geometry optimisations result in 0 K structures, which cannot account for thermal motion.

Table S1: Geometry optimisation information

Structure	RMSD (non-H) / Å	Maximum Displacement / Å	Displaced Atom
FOCCAD	**0.347**	2.039	H15
VAGKUM_A	0.179	1.003	H2N3
VAGKUM_B	0.141	0.778	H1W
WOCPEM	0.041	0.825	H13A
WOCPEM NEW	0.093	0.826	H3AB

3. Crystal Structure Visualisation

Visualisations were created using either Mercury (Version 5.3.0)[1] or Olex2 (Version 1.3).[7]

(a)

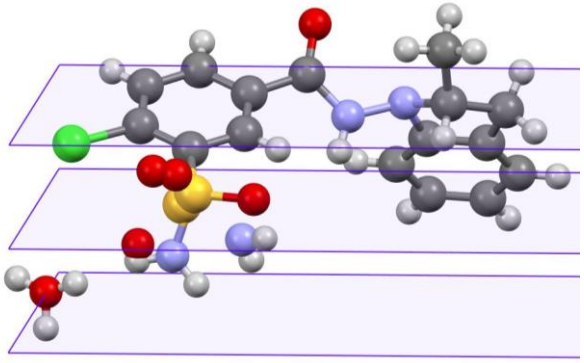

(b)

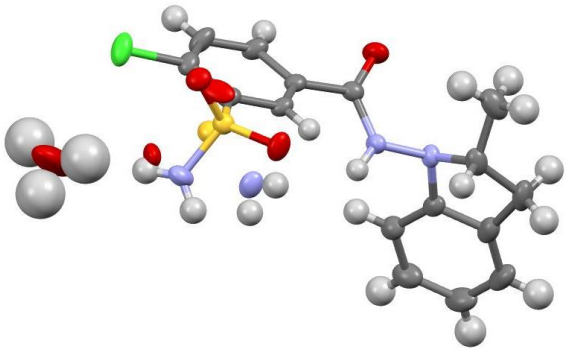

Figure S3: The asymmetric unit of **VAGKUM** with (a) the glide planes visualised in purple and (b) the anisotropic ADPs visualised. Note the chemically implausible water molecule resulting from the "disorder by symmetry".

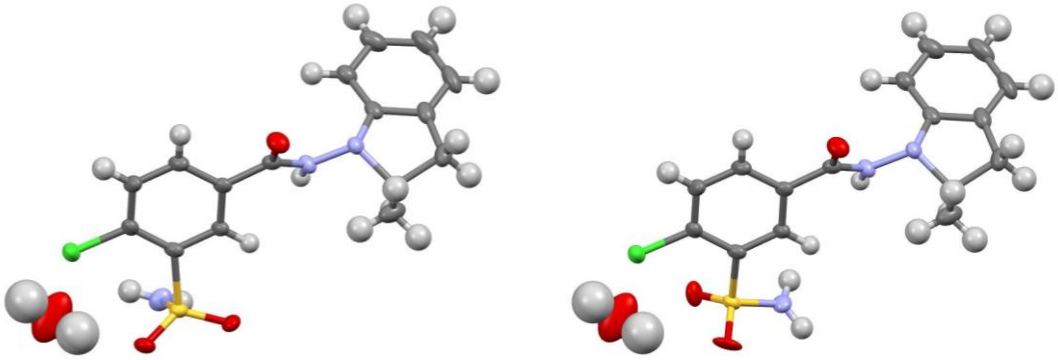

VAGKUM_A **VAGKUM_B**

Figure S4: Illustration of the disordered sulfonamide group positions in **VAGKUM**, including the anisotropic ADPs. The disorder is described as 50:50 disorder within the CIF, with involved atoms labelled either B1 (VAGKUM_A) or B2 (VAGKUM_B).

(a) Asymmetric Unit

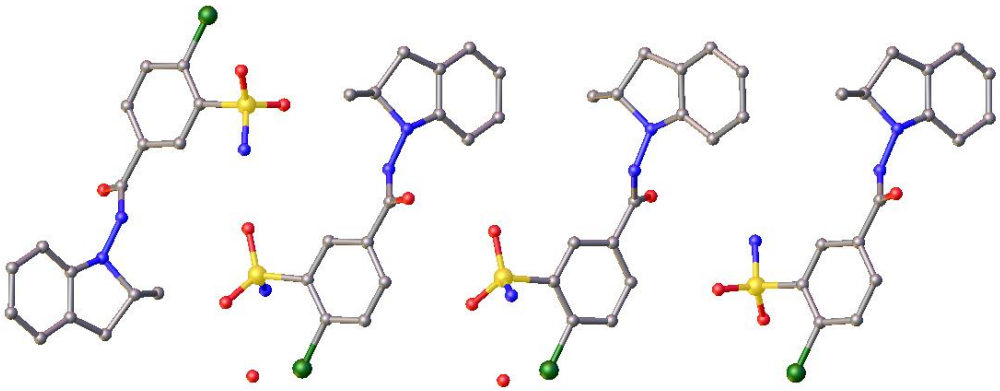

(b) Anisotropic ADPs

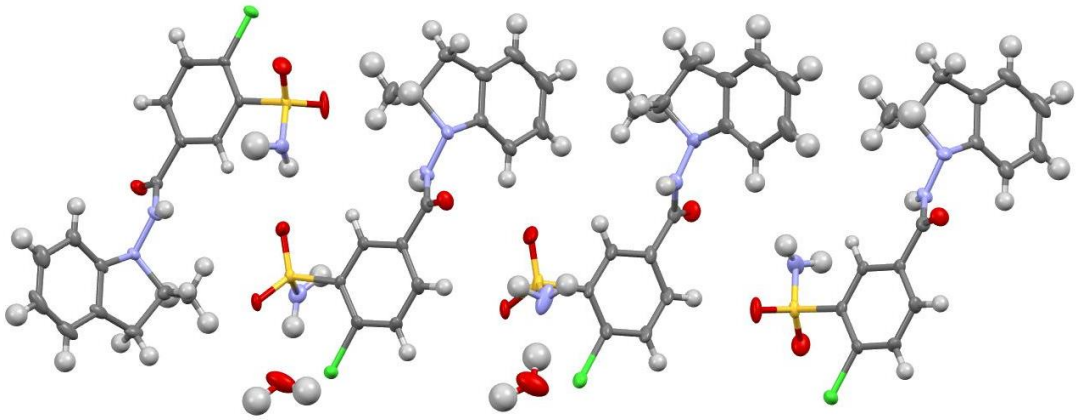

(c) Packing

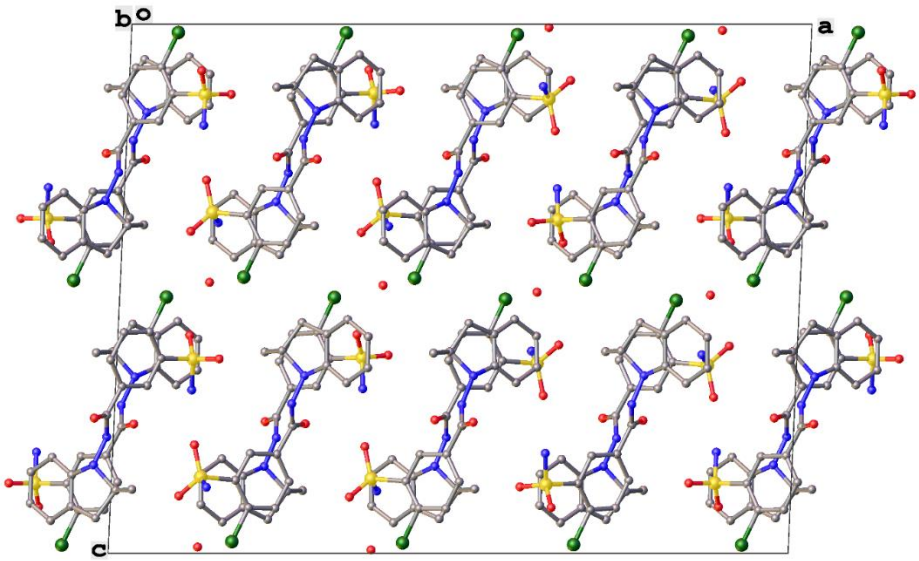

Figure S5: (a) Asymmetric unit along the 010 plane, (b) anisotropic ADPs and (c) packing of **WOCPEM NEW.**

4. Solid-State NMR

Indapamide hemihydrate (IND) was purchased from Merck Life Sciences Ltd and used without further purification.

SSNMR experiments were performed using an Oxford 11.7 T superconducting magnet, and a Bruker AVANCE III HD console, operating at frequencies of 499.69 (^{1}H) and 125.65 (^{13}C) MHz. The data was collected using a 4 mm HX magic-angle spinning probe at ambient temperature. The ^{13}C chemical shifts were referenced using the high-frequency signal of adamantane ($\delta_{iso}(^{13}C)$ = 38.5 ppm). SPINAL64 heteronuclear decoupling[8] was used during acquisition with a ^{1}H nutation frequency of approximately 73.5 kHz. The resulting spectrum agreed well with previously published data.[9]

Table S2: Experimental Solid-State NMR Details

Nucleus	^{13}C
Experiment Type	CP/TOSS[10]
Spectral Width / kHz	50
Number of Points	4994
^{1}H 90° / µs	3.4
^{13}C 90° / µs	4.0
Number of Scans	512
Recycle Delay / s	7.0
Contact Time / ms	1.0
MAS Frequency / kHz	9.0

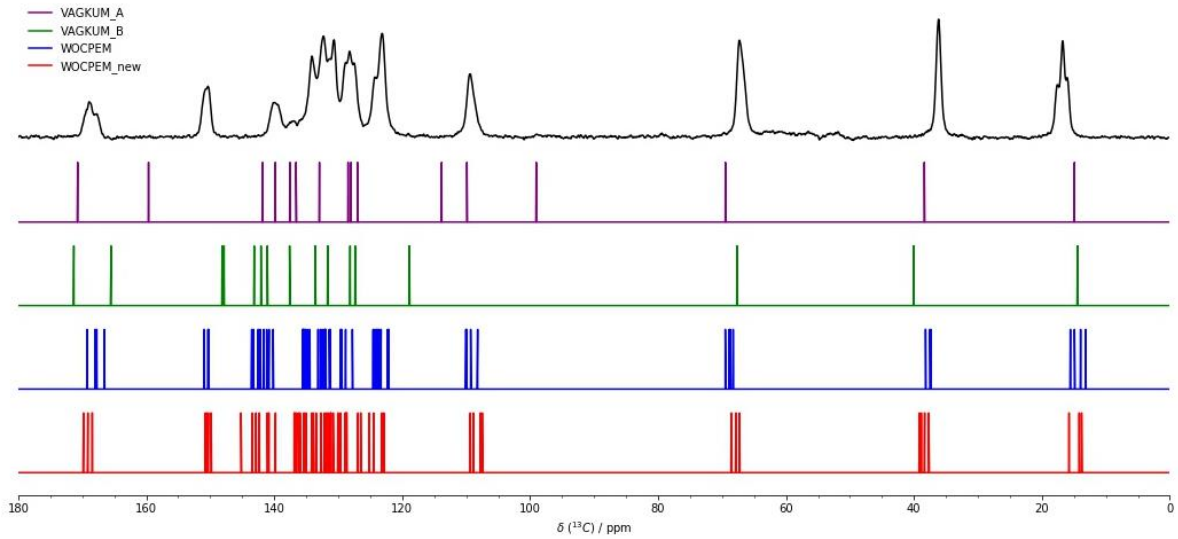

Figure S6: Comparison of calculated ^{13}C chemical shifts for **VAGKUM_A** (purple), **VAGKUM_B** (green), **WOCPEM** (blue) and **WOCPEM NEW** (red) with the acquired experimental data (black). As noted

below, the unphysical structures of the **VAGKUM** structures means that that the **VAGKUM** results should be interpreted with caution.

5. Computational Methods

First principle calculations were carried out using the GIPAW method implemented into CASTEP version 17.2/19.1,[11] using the Perdew, Burke and Ernzerhof (PBE) functional and on-the-fly generated ultrasoft pseudopotentials.[12,13] Integrals were taken over the Brillouin zone using a Monkhorst-Pack grid.[14] Unless specified otherwise, the maximum k-point spacing was 0.1 $Å^{-1}$ and a k-point offset of (¼, ¼, ¼) was used. All atomic positions were geometry optimised with the centre of mass and unit cell parameters fixed at their diffraction-determined values. Input files were generated using CIF2cell[15], with the original CIF labelling incorporated into the output magres files.[16] NMR parameters were calculated[17,18] using the same parameters, and the resulting ^{13}C shielding values were converted to chemical shifts using a subset of ^{13}C resonances that could be unambiguously assigned in the experimental data. As shown in Figure 2, there appears to be systematic deviations in the alkyl region. One method of mitigation is split scale referencing[19] however, this becomes unfeasible with the limited number of data points. Another explanation is the sensitivity of methyl carbons to nuclear quantum effects where decreases of up to 20 ppm for calculated shieldings have been observed.[20]

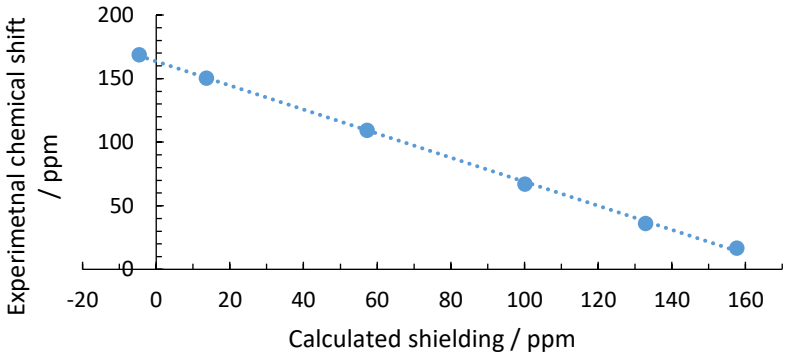

Figure S7: Correlation between the calculated shieldings of **WOCPEM** vs. experimental isotropic chemical shifts for a subset of six clearly assigned carbons. All atomic positions were DFT optimised prior to the NMR calculation. The blue dashed line from linear regression corresponds to a gradient of –0.9458 and a σ_{ref} of 163.5 ppm. Corresponding correlations were determined for **VAGKUM_A** (gradient of –1.0318, σ_{ref} of 172.2 ppm), **VAGKUM_B** (gradient of –1.0052, σ_{ref} of 173.2 ppm) and **WOCPEM NEW** (gradient of –0.9489, σ_{ref} of 164.4 ppm).

Due to the 50:50 disorder on the sulfonamide group, the **VAGKUM** structure was resolved into two separate CIFs corresponding to the different sulfonamide orientations (**Figure S3**), retaining the same unit cell. The pseudo symmetry of the water molecule could not be resolved in this way, and the virtual crystal approximation[21] (VCA) was used to model the 50% occupancy of the two H positions. This was a pragmatic choice that which allowed the calculations to be performed despite the disorder. This means that the results from **VAGKUM**, particularly for sites close to the water molecule, should be interpreted cautiously.

WOCPEM and **WOCPEM NEW** have very large unit cells so some modifications were required to allow the calculations to be performed on the local high-performance-computing cluster. Since the k-point grid was 2 × 1 × 1, the k-point grid offset could be safely removed and symmetry used to perform the

calculation on a single k-point at (½, 0, 0), which crucially is not the Γ point, (0, 0, 0). Secondly, "node dilution" was used to increase the amount of memory available to each compute task; the number of tasks allocated to each node was dropped from 24 processes to 18, which allowed the 54 GB of memory per compute node to be used effectively.

6. Quantitative Assessment of Agreement

The chemical shifts calculated for **WOCPEM** were averaged over $Z' = 4$, scaled using the referencing from **Figure S8**, and somewhat simplistically assigned to the experimental chemical shifts in the 1D ^{13}C spectrum by assuming that the order of computed and calculated shifts is the same. Hence, the overall RMSD of 1.70 ppm is likely to be an underestimate.

Table S3: Simplistic Partial Assignment of ^{13}C Chemical Shifts of IND.

Carbon Number	Experimental Chemical Shift / ppm	Calculated Chemical Shift / ppm	Difference / ppm
C9	168.89	167.98	0.91
C4	150.43	150.94	–0.51
C12	139.86	143.24	–3.38
C13	139.86	141.64	–1.78
C5	109.36	109.29	0.07
C1	67.23	68.83	–1.60
C2	36.21	37.36	–1.15
C16	16.8	14.90	1.90
		RMSD	**1.70**

7. Lineshape Analysis

The open-source software, ssNake (Version 1.3)[22] was used to fit the lineshapes of the C=O and Me signals. Using the standard parameters of the software (**Table S4A**), the overall lineshape for each peak was fitted to four component signals with a common lineshape and integral (**Table S4B**).

Table S4A: ssNake parameters used in the lineshape analysis for the Me and C=O signals.

Min. Method	Powell
Significant Digits	4
Number of Evaluations	500
Fitting Method	Lorentzian/Gaussian

Table S4B: Fitted chemical shift values for the Me and C=O signals analysed using ssNake.

Environment	Me				CO			
	1	**2**	**3**	**4**	**1**	**2**	**3**	**4**
Fitted Chemical Shift / ppm	16.02	16.76	16.80	17.64	167.7	168.6	168.9	169.5
Integral	1.78e+10				8.88e+09			
Lorentz / Hz	83.3				114.0			
Gauss / Hz	25.3				19.8			

8. Crystallography

Prior literature described the use of slow evaporation to obtain suitable X-ray crystals. Bojarska et al. describe using a hexane-acetonitrile solution to obtain suitable crystals (**VAGKUM**) after a period of several weeks[2] whilst Aljohani et al. rather accidentally produced suitable crystals from an attempted cocrystallisation of IND with gliclazide in methanol (**WOCPEM**).[3] Both conditions were attempted. The **VAGKUM** conditions failed to produce suitable crystals, but suitable crystals for SCXRD were grown from the **WOCPEM**-like conditions. 10 mL of methanol was used and the resulting solution was left to evaporate at room temperature for approximately two weeks.

The crystal was mounted on a Microloop 300 (MiTiGen Inc.) holder using Fomblin oil (Solvay Solexis). The X-ray single crystal data have been collected using λMoKα radiation (λ = 0.71073 Å) on a Bruker D8Venture (Photon III MM C14 CPAD detector, Incoatec IμS-3.0 microsource, focusing mirrors) 3-circle diffractometer equipped with a Cryostream (Oxford Cryosystems) open-flow nitrogen cryostat at the temperature 120.0(2) K. The frames were integrated using SAINT V8.40A (Bruker, 2019); SADABS V2012/1 (Bruker AXS Inc.) was used for scaling and absorption correction. The structure was solved by direct method and refined by full-matrix least squares on F^2 for all data using Olex2[7] and SHELXTL[23] software. All non-hydrogen atoms were refined in anisotropic approximation. C-bound hydrogen were placed in the calculated positions and refined in riding mode; N- and O-bound hydrogen atoms were located in a difference Fourier map and refined isotropically. Crystallographic data for the structure have been deposited with the Cambridge Crystallographic Data Centre as supplementary publication CCDC-2115849.

Table S5: Crystallographic details for WOCPEM NEW structure

Empirical formula	$C_{16}H_{17}ClN_3O_{3.5}S$
Formula weight / g mol^{-1}	374.83
Temperature / K	120
Crystal system	monoclinic
Space group	$P2_1/c$
a / Å	30.1401(10)
b / Å	9.6025(4)
c / Å	23.4611(8)
α / °	90
β / °	92.5930(10)
γ / °	90
Volume / Å^3	6783.2(4)
Z	16
ρ_{calc} / g cm^{-3}	1.468
μ / mm^{-1}	0.372

F(000)	3120.0
Crystal size / mm^3	0.34 × 0.12 × 0.05
Radiation	MoKα (λ = 0.71073 Å)
2Θ range for data collection / °	3.786 to 58
Index ranges	$-41 \le h \le 41$, $-13 \le k \le 13$, $-32 \le l \le 32$
Reflections collected	143804
Independent reflections	18001 [R_{int} = 0.0994, R_{sigma} = 0.0575]
Data/restraints/parameters	18001/61/979
Goodness-of-fit on F^2	1.127
Final *R* indexes [I>=2σ(I)]	R_1 = 0.0842, wR_2 = 0.1927
Final *R* indexes [all data]	R_1 = 0.1170, wR_2 = 0.2080
Largest diff. peak/hole / e Å^{-3}	0.88/–0.62

9. Research Data Bundle

A summary of data collated in the associated research data archive is described below with further comments in the README.txt.

Table S6: Summary of associated data in the IND Research Data

Research Data	Comments
XRD	Contains: • WOCPEM NEW.cif • WOCPEM NEW.hkl • WOCPEM NEW CheckCIF.pdf • Raw PXRD Data
Magres	Contains the .magres files for: • VAGKUM A • VAGKUM B • WOCPEM • WOCPEM NEW
Referencing.xlsx RMSD.xlsx	Linear scaling of calculated chemical shifts for: • VAGKUM A • VAGKUM B • WOCPEM • WOCPEM NEW RMSD calculation conducted using **WOCPEM**
NMR_Data_IND.py	Python script to produce Fig 2.
Indapamide.jdx and IND_fid	Raw and processed data for ^{13}C CP/TOSS experiment.

References

1. C. F. MacRae, I. Sovago, S. J. Cottrell, P. T. A. Galek, P. McCabe, E. Pidcock, M. Platings, G. P. Shields, J. S. Stevens, M. Towler and P. A. Wood, *J. Appl. Crystallogr.*, 2020, **53**, 226–235.
2. J. Bojarska, A. Fruziński and W. Maniukiewicz, *J. Mol. Struct.*, 2016, **1116**, 22–29.
3. M. Aljohani, P. MacFhionnghaile, P. McArdle and A. Erxleben, *Int. J. Pharm.*, 2019, **561**, 35–42.
4. A. A. Coelho, J. Evans, I. Evans, A. Kern and S. Parsons, *Powder Diffr.*, 2011, **26**, S22–S25.
5. J. Van De Streek and M. A. Neumann, *Acta Crystallogr. Sect. B Struct. Sci.*, 2010, **66**, 544–558.
6. C. M. Widdifield, J. D. Farrell, J. C. Cole, J. A. K. Howard and P. Hodgkinson, *Chem. Sci.*, 2020, **11**, 2987–2992.
7. O. V. Dolomanov, L. J. Bourhis, R. J. Gildea, J. A. K. Howard and H. Puschmann, *J. Appl. Crystallogr.*, 2009, **42**, 339–341.
8. B. M. Fung, A. K. Khitrin and K. Ermolaev, *J. Magn. Reson.*, 2000, **142**, 97–101.
9. L. M. Rus, I. Kacso, G. Borodi, M. Aluas, I. Tomuta, C. Iuga, S. Simon, I. Bratu and M. Bojita, *AIP Conf. Proc.*, 2012, **1425**, 39–42.
10. W. T. Dixon, J. Schaefer, M. D. Sefcik, E. O. Stejskal and R. A. McKay, *J. Magn. Reson.*, 1982, **49**, 341–345.
11. S. J. Clark, M. D. Segall, C. J. Pickard, P. J. Hasnip, M. I. J. Probert, K. Refson and M. C. Payne, *Z. Kristallogr.*, 2005, **220**, 567–570.
12. J. P. Perdew, K. Burke and M. Ernzerhof, *Phys. Rev. Lett.*, 1996, **77**, 3865-3868.
13. D. Vanderbilt, *Phys. Rev. B*, 1990, **41**, 7892-7895.
14. H. J. Monkhorst and J. D. Pack, *Phys. Rev. B: Condens. Matter Mater. Phys.* 1976, **13**, 5188–5192.
15. T. Björkman, *Comput. Phys. Commun.*, 2011, **182**, 1183–1186.
16. S. Sturniolo, T. F. G. Green, R. M. Hanson, M. Zilka, K. Refson, P. Hodgkinson, S. P. Brown and J. R. Yates, *Solid State Nucl. Magn. Reson.*, 2016, **78**, 64–70.
17. C. J. Pickard and F. Mauri, *Phys. Rev. B - Condens. Matter Mater. Phys.*, 2001, **63**, 245101.
18. J. R. Yates, C. J. Pickard and F. Mauri, *Phys. Rev. B - Condens. Matter Mater. Phys.*, 2007, **76**, 024401.
19. A. L. Webber, L. Emsley, R. M. Claramunt and S. P. Brown, *J. Phys. Chem. A*, 2010, **114**, 10435–10442.
20. M. Dračínský and P. Hodgkinson, *Chem. - A Eur. J.*, 2014, **20**, 2201–2207.
21. L. Bellaiche and D. Vanderbilt, *Phys. Rev. B.*, 2000, **61**, 7877–7882.
22. S. G. J. van Meerten, W. M. J. Franssen and A. P. M. Kentgens, *J. Magn. Reson.*, 2019, **301**, 56–66.
23. G. M. Sheldrick, *Acta Crystallogr. Sect. C Struct. Chem.*, 2015, **71**, 3–8.